Developmental Cell
Article

Lypd6 Enhances Wnt/β-Catenin Signaling by Promoting Lrp6 Phosphorylation in Raft Plasma Membrane Domains

Günes Özhan,[1] Erdinc Sezgin,[1] Daniel Wehner,[1,2] Astrid S. Pfister,[2] Susanne J. Kühl,[2] Birgit Kagermeier-Schenk,[1] Michael Kühl,[2] Petra Schwille,[1,3] and Gilbert Weidinger[1,2,*]
[1]Biotechnology Center, Technische Universität Dresden, Tatzberg 47, 01307 Dresden, Germany
[2]Institute for Biochemistry and Molecular Biology, Ulm University, Albert-Einstein-Allee 11, 89081 Ulm, Germany
[3]Max-Planck Institute of Biochemistry, Am Klopferspitz 18, 82152 Martinsried, Germany
*Correspondence: gilbert.weidinger@uni-ulm.de
http://dx.doi.org/10.1016/j.devcel.2013.07.020

SUMMARY

Wnt/β-catenin signaling plays critical roles during embryogenesis, tissue homeostasis, and regeneration. How Wnt-receptor complex activity is regulated is not yet fully understood. Here, we identify the Ly6 family protein LY6/PLAUR domain-containing 6 (Lypd6) as a positive feedback regulator of Wnt/β-catenin signaling. *lypd6* enhances Wnt signaling in zebrafish and *Xenopus* embryos and in mammalian cells, and it is required for *wnt8*-mediated patterning of the mesoderm and neuroectoderm during zebrafish gastrulation. Lypd6 is GPI anchored to the plasma membrane and physically interacts with the Wnt receptor Frizzled8 and the coreceptor Lrp6. Biophysical and biochemical evidence indicates that Lypd6 preferentially localizes to raft membrane domains, where Lrp6 is phosphorylated upon Wnt stimulation. *lypd6* knockdown or mislocalization of the Lypd6 protein to nonraft membrane domains shifts Lrp6 phosphorylation to these domains and inhibits Wnt signaling. Thus, Lypd6 appears to control Lrp6 activation specifically in membrane rafts, which is essential for downstream signaling.

INTRODUCTION

Wnt/β-catenin signaling controls embryonic development via regulation of cell proliferation, cell-fate determination, and tissue patterning in many species from cnidarians to mammals. It is also required for maintenance of adult tissue homeostasis and regeneration of various tissues and organs (Clevers, 2006; Logan and Nusse, 2004). Misregulation of Wnt/β-catenin signaling can cause congenital disorders, cancer, degenerative diseases, and other human conditions (MacDonald et al., 2009). During vertebrate gastrulation, β-catenin signaling activated by *wnt8* or *wnt3a* is essential for patterning of the mesoderm along the dorsoventral axis and of the neuroectoderm along the anteroposterior axis (Lekven et al., 2001; Yamaguchi, 2001). In fish and frogs, *wnt8* induces the formation of ventral and lateral mesoderm and restricts the dorsal organizer, while it posteriorizes the neuroectoderm, allowing for the formation of hindbrain and spinal cord. Both patterning events need to be precisely regulated and thus are tightly controlled by several proteins that act as Wnt signaling modifiers.

In the absence of pathway-activating ligands, β-catenin is phosphorylated by Glycogen synthase kinase 3 (Gsk3) and Casein kinase 1 (Ck1) in a cytoplasmic protein complex that also includes Axin and Adenomatous polyposis coli (Apc). Phosphorylated β-catenin is degraded by the ubiquitin-proteasome pathway (Kimelman and Xu, 2006). Signaling is initiated by the interaction of Wnt ligands with Frizzled (Fz) receptors and the coreceptors low density lipoprotein receptor-related proteins 5/6 (Lrp5/6) (Angers and Moon, 2009). One early response to ligand-receptor interaction is phosphorylation of the intracellular domain of Lrp5/6 at serine and threonine residues by Gsk3 and Ck1 (Angers and Moon, 2009; MacDonald et al., 2009). Consequently, the cytoplasmic scaffolding protein Dishevelled (Dvl) and Axin are recruited to the receptors, resulting in inhibition of the degradation complex, which leads to stabilization and nuclear translocation of β-catenin. Here, β-catenin modifies expression of target genes together with transcription factors of the lymphoid enhancer-binding factor (Lef) and T cell factor (Tcf) family (Angers and Moon, 2009; MacDonald et al., 2009). Although numerous additional components of the Wnt/β-catenin pathway have been characterized, many questions related to the tight regulation and modification of signaling remain unanswered.

Lrp6 phosphorylation and endocytosis of receptor complexes are both necessary steps in activation of Wnt/β-catenin signaling, and they appear to occur independently of each other (Kikuchi and Yamamoto, 2007; Niehrs and Shen, 2010; Yamamoto et al., 2008). Whereas Lrp6 is distributed throughout the plasma membrane, its phosphorylation specifically occurs in liquid-ordered membrane domains, so-called rafts (historically often referred to as lipid rafts) (Sakane et al., 2010; Yamamoto et al., 2008). Rafts are currently thought of as highly dynamic membrane nanodomains that can be stabilized and enlarged by formation of protein clusters, e.g., via stimulation of receptor clustering by ligands, and thus function to compartmentalize the plasma membrane and act as platforms for interaction of signaling molecules (Kusumi et al., 2012). Rafts can be endocytosed as caveolae, and Wnt ligands have been shown to induce the internalization of Lrp6 with Caveolin, whereas the pathway inhibitor Dickkopf-1 (Dkk1) removes Lrp6 from rafts

and causes its internalization with Clathrin (Sakane et al., 2010). Thus, Lrp6 phosphorylation in raft membrane domains and subsequent internalization into signaling-competent vesicles appear to be essential for Wnt pathway activation. How raft-specific Lrp6 phosphorylation is regulated is, however, unknown.

Here, we identify *LY6/PLAUR domain-containing 6* (*lypd6*), coding for a member of the Ly6 protein family, as a transcriptional target of Wnt/β-catenin signaling during zebrafish embryogenesis. The Ly6 family of proteins comprises low molecular weight molecules that are either secreted or glycophosphatidylinositol (GPI) anchored to the cell surface and are characterized by presence of one or more conserved LU domain(s), whose molecular function is unknown (Kong and Park, 2012). Functionally, the Ly6 family is very diverse, including immunomodulatory molecules like Cd59, the urokinase plasminogen activator receptor (uPar), and regulators of cell migration, adhesion, and proliferation (Bamezai, 2004; Gumley et al., 1995). Only a few Ly6 family members have been implicated in embryonic development, including *Drosophila leaky/coiled*, in establishment of the blood-brain barrier, and *Drosophila twit*, in regulation of neurotransmitter release at the developing neuromuscular junction (Kim and Marqués, 2012; Syed et al., 2011). Little is known about *lypd6*, the Ly6 member characterized here.

We show that *lypd6* acts as a feedback enhancer of β-catenin signaling during zebrafish gastrulation. Lypd6 is GPI anchored to the plasma membrane and partitions into raft membrane domains. Moreover, our data suggest that Lypd6 promotes Wnt signaling by ensuring phosphorylation of Lrp6 specifically in rafts. Thus, we propose that Lypd6 is part of a molecular machinery that facilitates efficient Wnt receptor complex activation in plasma membrane domains that are competent to transmit the signal to the interior of the cell via internalization into signaling-competent vesicles.

RESULTS

lypd6 Is Transcriptionally Regulated by Wnt/β-Catenin Signaling

To discover modulators of Wnt/β-catenin signaling, we took advantage of the fact that many Wnt pathway components are transcriptionally regulated by the pathway itself (MacDonald et al., 2009). Thus, we performed gene expression profiling of zebrafish embryos after conditional activation and inhibition of β-catenin signaling at gastrula, somitogenesis, and organogenesis stages and screened for genes positively regulated by the pathway during at least two developmental stages (Kagermeier-Schenk et al., 2011; B.K.-S. and G.W., unpublished data). Among such broadly regulated genes, we identified *LY6/PLAUR domain-containing 6* (*lypd6*), whose function during vertebrate embryonic development has not been described.

In the course of zebrafish development, *lypd6* expression was initially detected in mesendodermal cells at late blastula stages (Figure S1A available online). During gastrulation, it was expressed in a broad marginal domain (Figure S1B) and became excluded from the ventral animal pole at late gastrula stages (Figure 1A). During segmentation, *lypd6* was initially exclusively detected in the somitic mesoderm (Figure 1A) but later also in the otic and optic vesicles (Figure S1C). During organogenesis, expression was largely downregulated in the somites but maintained in the otic vesicles and the retina (Figure S1D). A *Xenopus lypd6* homolog (*xlypd6*) showed a similar expression pattern. *xlypd6* was initially detected at the animal pole of blastula stages (Figures S1E and S1F) and expressed in the expanding ectoderm and mesoderm during gastrulation (Figures S1G and S1H) and in the neural plate during neurulation (Figures S1I and S1J). During tailbud stage, *xlypd6* was expressed in the head region (Figure S1K) and in the somites (Figure S1L). Analyses of tailbud tissue sections revealed *xlypd6* expression in anterior neural crest cells, lens, otic vesicles, and dermatomes of the somites (Figures S1M–S1P).

Overexpression of the β-catenin pathway inhibitors Axin1 or Dkk1 for 3 hr in heat-shock-inducible *hsp70l*:Mmu.Axin1-YFP^{w35} (*hs*:Axin1; Kagermeier-Schenk et al., 2011) and *hsp70l*:Dkk1b-GFP^{w32} (*hs*:Dkk1; Stoick-Cooper et al., 2007) transgenic zebrafish embryos suppressed *lypd6* expression at gastrula and somitogenesis stages (Figure 1A). These results were verified by qRT-PCR, which also revealed that activation of β-catenin signaling via *wnt8* overexpression in *hsp70l*:Wnt8a-GFP^{w34} (*hs*:Wnt8; Weidinger et al., 2005) transgenic embryos was sufficient to significantly upregulate *lypd6* expression during somitogenesis (Figure 1B). Hence, we conclude that *lypd6* is a transcriptional target of Wnt/β-catenin signaling in several tissues during zebrafish development, suggesting that it could act as a feedback modifier of the pathway.

Lypd6 Is GPI Anchored to the Plasma Membrane

Lypd6 belongs to the Ly6 family of proteins that is characterized by an LU domain with conserved cysteine residues and contains proteins of highly diverse functions. Ly6 proteins are either secreted or glycophosphatidylinositol anchored to the plasma membrane (Bamezai, 2004; Gumley et al., 1995). Bioinformatic analyses showed that the predicted zebrafish Lypd6 protein sequence contains both a potential signal peptide sequence (Figure S1Q) and a potential C-terminal GPI anchor attachment site, referred to as the omega site (Figure S1R). To verify Lypd6's subcellular localization, we generated a tagged construct by inserting GFP between the signal peptide (sp) and the rest of the protein (spGFP-Lypd6, Figure 1C). This construct localized to the plasma membrane, both in zebrafish embryos and cultured mammalian cells, whereas a truncated version lacking the C-terminal domain that contains the omega site (spGFP-Lypd6ΔGPI) did not (Figures 1C and 1D). In line with this, spGFP-Lypd6 and a spGFP-GPI control construct could not be detected in the media conditioned by transfected cells, whereas spGFP-Lypd6ΔGPI and a spGFP control construct could (Figure 1E). However, when cells were treated with Phosphatidylinositol-specific phospholipase C (PIplC), which cleaves the GPI anchor of cell-surface proteins, both spGFP-GPI and spGFP-Lypd6 were detected in the media (Figure 1E). These data indicate that Lypd6 localizes to the plasma membrane via a GPI anchor.

lypd6 Enhances Wnt/β-Catenin Signaling

To examine a potential role of *lypd6* in Wnt/β-catenin signaling, we first asked whether it can modify the distinctive phenotypes caused by *wnt8* overexpression in zebrafish embryos (Lekven et al., 2001). With increasing signaling strength, these phenotypes range from mild posteriorization of the neuroectoderm to loss of notochord (classes 1 to 4, Figure 2A). We induced

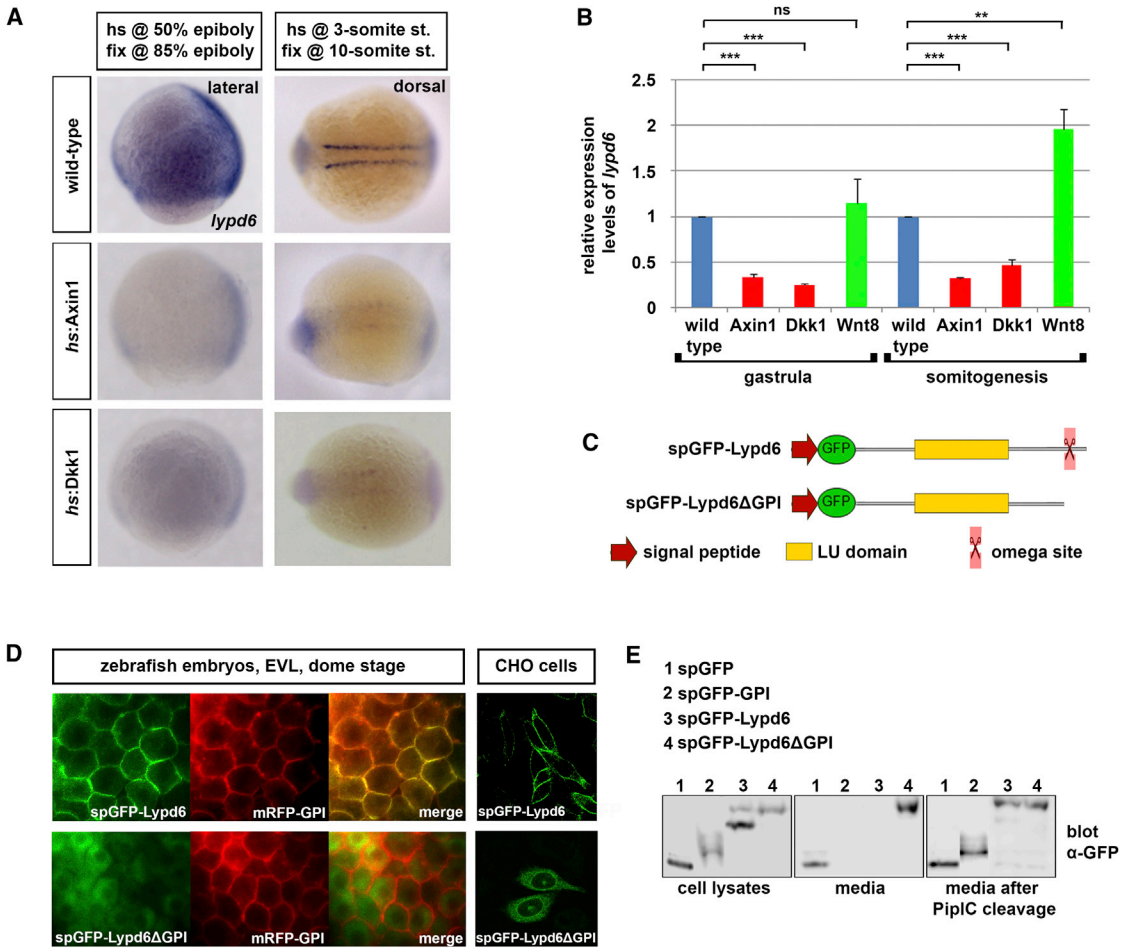

Figure 1. Zebrafish *lypd6* Is a Wnt/β-Catenin Target Gene that Codes for a GPI-Anchored Plasma Membrane Protein

(A) *lypd6* whole-mount in situ hybridization (WMISH) showing downregulation in transgenic embryos expressing Axin1 or Dkk1 at gastrula and somitogenesis stages (n [85% epiboly]: Axin1 16/17 embryos, Dkk1 19/19; n [10-somites]: Axin1 21/21, Dkk1 18/18). hs, heat shock.

(B) *lypd6* expression levels determined by qRT-PCR in *hs*:Axin1, *hs*:Dkk1, and *hs*:Wnt8 transgenic embryos treated as in (A) and shown relative to those in wild-type embryos. Error bars, SEM.

(C) Domain structure of N-terminally GFP-tagged wild-type (spGFP-Lypd6) and C-terminally truncated Lypd6 (spGFP-Lypd6ΔGPI).

(D) Localization of spGFP-Lypd6 and spGFP-Lypd6ΔGPI in enveloping layer (EVL) cells of dome stage zebrafish embryos and in Chinese hamster ovary (CHO) cells.

(E) Release of spGFP-Lypd6 and spGFP-GPI from the plasma membrane of HEK293T cells upon treatment with phosphatidylinositol-specific phospholipase C (PIPLC). spGFP-Lypd6ΔGPI and spGFP are detectable in the conditioned media without PIPLC treatment.

See also Figure S1.

β-catenin signaling in *hs*:Wnt8 transgenic embryos by applying a single heat shock at early gastrula (shield stage), which consistently resulted in class 2 phenotypes at 24 hr postfertilization (hpf) (Figure 2B). Injection of *spGFP-lypd6* RNA significantly enhanced the phenotypes to class 3 and class 4, whereas *spGFP-lypd6ΔGPI* had no effect (Figure 2B). Similarly, *lypd6* RNA worsened the phenotypes caused by *wnt8* RNA injection as assayed by marker gene expression at early somitogenesis stages (Figures S2A and S2B). Moreover, *spGFP-lypd6* augmented Wnt3a-induced expression of the pBAR reporter of Tcf/Lef-mediated transcription (Biechele and Moon, 2008) in cultured human embryonic kidney (HEK) 293T cells, whereas *spGFP-lypd6ΔGPI* did not (Figure 2C). Finally, zebrafish *lypd6* synergized with *wnt3a* in secondary axis induction assays in *Xenopus* embryos, where low doses of *wnt3a* plus *lypd6* induced significantly more complete secondary axes than *wnt3a* plus control RNA (Figures S2C and S2D). Of note, *lypd6* was not sufficient on its own to activate β-catenin signaling in any of these assays. Together, these results show that *lypd6* has the ability to enhance Wnt/β-catenin signaling, which requires its GPI anchorage to the cell surface.

Next, we asked whether endogenous *lypd6* is necessary for Wnt/β-catenin signaling in zebrafish embryos using antisense morpholino oligonucleotide (MO)-mediated knockdown. Injection of a translation-blocking MO against *lypd6* caused a reduction in size of trunk and tail, and this phenotype was robustly rescued by coinjection of *lypd6* RNA that could not be bound by the MO (Figure 2D). Posterior truncations were also evident

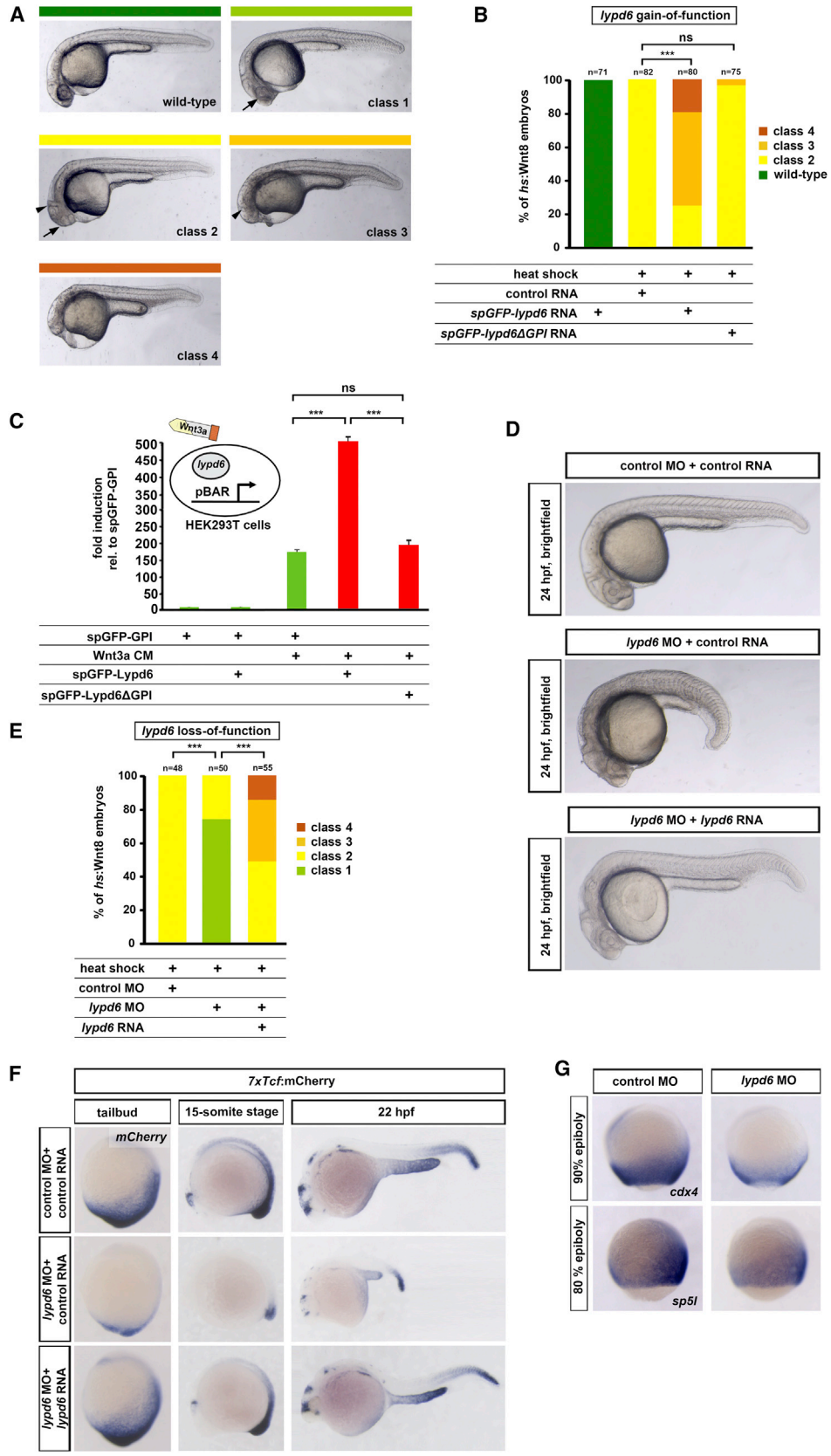

(legend on next page)

by a reduction in the total number of somites and fusion of posterior somites marked by the expression of the somitic marker *myoD* (Figure S2E, number of somites = 28 ± 1 control, 20 ± 3 *lypd6* MO). This phenotype is similar to the morphological effect on the trunk and tail produced by the knockdown of *wnt8* (Figure S2E, 17 ± 2 somites; Lekven et al., 2001). Injection of *lypd6* MO into heat shocked *hs*:Wnt8 transgenic embryos significantly reduced the severity of phenotypes induced by Wnt8, whereas injection of the MO with *lypd6* RNA that could not be bound by the MO reversed the rescue and caused an enhancement of the *wnt8*-induced phenotypes (Figure 2E). These results indicate that *lypd6* is required for Wnt8-mediated exogenous and endogenous β-catenin signaling.

To further test whether *lypd6* is required for endogenous β-catenin signaling during zebrafish development, we monitored the effect of *lypd6* knockdown on expression of a transgenic reporter of Tcf/Lef-mediated transcription, *7xTcf-Xla.Siam:*nlsmCherry[ia] (*7xTcf*:mCherry; Moro et al., 2012). Reporter expression was dramatically reduced in *lypd6* morphants at late gastrula, somitogenesis, and organogenesis stages, and this downregulation was efficiently rescued by coinjection of *lypd6* RNA (Figure 2F). We found that *lypd6* knockdown had no effect on reporter activity at late blastula stages on the dorsal side (30% epiboly, 5 hpf), which is regulated by maternal β-catenin signaling. In contrast, at early gastrula (shield stage, 6 hpf) ventrolateral *mCherry* expression, which depends on zygotic *wnt8*-mediated signaling, was downregulated in *lypd6* morphants (Figure S2F). Thus, consistent with its expression starting after midblastula transition, *lypd6* appears to be required for activation of the earliest zygotic Wnt/β-catenin responses, but not for those dependent on maternal β-catenin. *lypd6* knockdown also caused a reduction in expression of the direct Wnt/β-catenin target genes *cdx4* and *sp5l* (Pilon et al., 2006; Weidinger et al., 2005) at gastrula stages (Figure 2G). In contrast, *lypd6* knockdown neither affected the ability of ectopic Fgf nor Nodal ligands to induce expression of targets genes of these pathways (Figures S2G and S2I). Thus, we conclude that *lypd6* predominantly acts as a modifier of Wnt/β-catenin signaling during zebrafish gastrulation.

lypd6 Is Required for *wnt8*-Mediated Mesoderm and Neuroectoderm Patterning

Prominent roles of *wnt8*-mediated β-catenin signaling during gastrulation are the specification of ventrolateral mesodermal fates and the restriction of the dorsal organizer (Lekven et al., 2001). Thus, we asked whether *lypd6* is necessary for mesodermal patterning of the embryo. *lypd6* knockdown resulted in a significant expansion of dorsal mesodermal fates marked by *goosecoid* (*gsc*), not at late blastula (30% epiboly), but at early gastrula (60% epiboly) stages (Figures 3A and 3B), suggesting that *lypd6* is required for *wnt8*-mediated organizer restriction. Although low doses of *wnt8* MOs or *lypd6* MO alone did not alter *gsc* expression, in combination they caused a severe expansion of the organizer domain, suggesting that *lypd6* genetically interacts with *wnt8* in mesoderm patterning (Figures 3C and 3E). Importantly, when injected at higher doses *wnt8* MOs strongly expanded the dorsal organizer, which was restored to the wild-type pattern by coinjection of *lypd6* RNA, indicating that *lypd6* can enhance residual *wnt8* signaling in the morphants (Figures 3D and 3E). These data suggest that *lypd6* acts as an essential positive modulator of *wnt8*-activated β-catenin signaling during dorsoventral mesoderm patterning.

Wnt/β-catenin signaling is also required in neuroectodermal patterning for induction of posterior neural fates during gastrulation. *lypd6* knockdown resulted in an expansion of the presumptive forebrain and the midbrain marked by *otx2* expression and in a corresponding reduction of the posterior neural region marked by *hoxb1b* (Figure 3F), suggesting that *lypd6* is required for neuroectodermal posteriorization. We conclude that *lypd6* is essential for the Wnt/β-catenin-controlled patterning of the mesoderm and neuroectoderm during zebrafish gastrulation.

lypd6 Acts in Wnt-Receiving Cells at the Level of the Wnt Receptor Complex

We next asked whether *lypd6* acts in Wnt-producing or Wnt-receiving cells. Knockdown of mouse *lypd6* transcripts via small interfering RNA (siRNA)-mediated gene silencing to about 27% (Figure S3A) in Wnt3a-secreting murine L cell fibroblasts did not reduce the pBAR-inducing activity of media conditioned by these cells (Figure 4A), indicating that *lypd6* is not required in Wnt-producing cells. In contrast, *lypd6* knockdown in pBAR-transfected L cells significantly reduced reporter activation by Wnt3a-conditioned media (Figure 4B), indicating that *lypd6* is required in Wnt-receiving cells. Likewise, siRNA- or endoribonuclease-prepared siRNA (esiRNA)-mediated knockdown of human *lypd6* to 23% (Figure S3B) or 5%, respectively (Figure S3C), significantly reduced Wnt3a-mediated pBAR activation also in HEK293T (Figures S3D and S3E) and RKO cells (Figure S3F). Furthermore, in zebrafish embryos transplantation of cells from *wnt8* RNA-expressing donors repressed the forebrain marker *otx2* in host embryos, and this ability was not altered when *lypd6* was knocked down in the donors

Figure 2. *lypd6* Enhances Wnt/β-Catenin Signaling

(A) Classification of phenotypes caused by *wnt8* overexpression in zebrafish embryos: class 1, small eyes (arrow); class 2, no eyes (arrow) but normal midbrain-hindbrain boundary (mhb) (arrowhead); class 3, severely reduced forebrain and midbrain and mhb not detectable (arrowhead); and class 4, loss of notochord.

(B) Phenotypes in *hs*:Wnt8 transgenic embryos injected with *spGFP-lypd6* RNA (150 pg), *spGFP-lypd6ΔGPI* (140 pg), or equimolar amounts of *spGFP-GPI* control RNA and heat shocked at shield stage and scored at 24 hpf.

(C) pBAR luciferase reporter activity normalized to renilla luciferase levels in Wnt3a CM-treated HEK293T cells transfected with spGFP-Lypd6 (100 ng), *spGFP-Lypd6ΔGPI* (95 ng), or equimolar amounts of spGFP-GPI control. Error bars, SEM.

(D) Morphological phenotypes at 24 hpf of embryos injected with *lypd6* MO (10 ng, 42/51 embryos) are rescued by coinjected *lypd6* RNA (150 pg, 49/58 embryos).

(E) Rescue of phenotypes in *hs*:Wnt8 embryos injected with *lypd6* MO (10 ng). Coinjected *lypd6* RNA (150 pg) restores the more severe phenotypes.

(F) Reduction of reporter activity in *7xTcf*:mCherry embryos injected with 10 ng *lypd6* MO plus 100 ng control RNA (n = 28/31). Coinjected *lypd6* RNA (75 ng) restores expression (n = 21/25).

(G) Downregulation of *cdx4* (90% epiboly, 19/20) and *sp5l* (80% epiboly, 13/15) in embryos injected with 10 ng *lypd6* MO.

See also Figure S2.

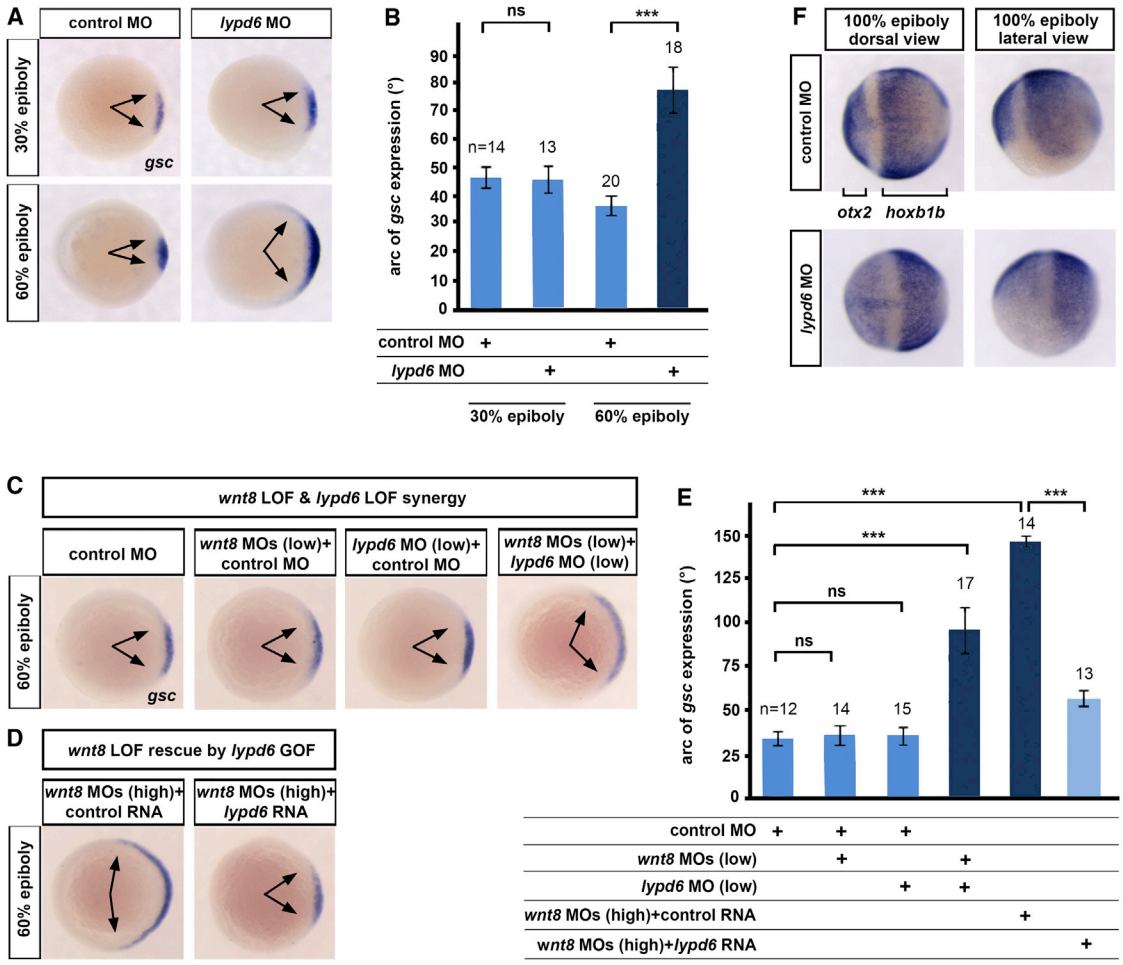

Figure 3. *lypd6* Is Necessary for *wnt8*-Mediated Mesoderm and Neuroectoderm Patterning

(A) Expansion of the dorsal organizer domain (arrows) marked by *goosecoid* (*gsc*), not at late blastula (30% epiboly), but at early gastrula (60% epiboly) stage in embryos injected with 10 ng *lypd6* MO.

(B) Quantification of the experiment shown in (A). Error bars, SEM.

(C) Changes in the size of the *gsc* expression domain (arrows) at 60% epiboly in embryos injected with low doses of *wnt8.1* and *wnt8.2* MOs (1.25 ng each) and *lypd6* MO (2 ng), relative to embryos injected with equimolar amounts of control MO.

(D) *gsc* expression in embryos injected with high doses of *wnt8* MOs (5 ng each) and 150 pg *lypd6* RNA or equimolar amounts of GFP control RNA.

(E) Quantification of the experiments shown in (C) and (D). Error bars, SEM.

(F) Expansion of the forebrain marker *otx2* and reduction of the posterior neural marker *hoxb1b* at the 100% epiboly stage in embryos injected with 10 ng *lypd6* MO (19/23).

(Figure S3G, middle row). In contrast, *wnt8*-expressing donor cells could not repress *otx2* in hosts in which *lypd6* was knocked down (Figure S3G, bottom row). Together, these data strongly suggest that *lypd6* has no role in Wnt production or secretion but is necessary for Wnt reception or signal transduction in Wnt-receiving cells.

To address at which position in the Wnt/β-catenin pathway *lypd6* acts, we inhibited signaling at different levels in the *7xTcf*:mCherry Wnt reporter line and asked whether *lypd6* coexpression could reverse loss of reporter expression. *lypd6* RNA efficiently restored the reporter expression inhibited by *wnt8* MOs, although it could not rescue the inhibition caused by *axin1* or *gsk3β* overexpression at the level of the β-catenin degradation complex or by the dominant-negative *tcf3*, *tcf3ΔC*, at the transcriptional level (Figure 4C). These findings indicate that *lypd6* enhances Wnt/β-catenin signaling upstream of the β-catenin degradation complex.

Lypd6 Directly Interacts with Lrp6 Independently of Its GPI Anchor

Because Lypd6 is localized to the plasma membrane, we asked whether it physically interacts with members of the Wnt receptor complex. Lypd6 coimmunoprecipitated (coIPed) with Lrp6, but not with the Ldl receptor (Ldlr), which is related to Lrp6 but has no role in β-catenin signaling (Figure 5A, lanes 2 and 3). In contrast, Lypd6 lacking the GPI attachment site did not interact with Lrp6 (Figure 5A, lane 5). However, a construct in which the GPI anchor attachment site was replaced with the transmembrane domain (TMD) of human CD44 (spGFP-Lypd6ΔGPI-CD44 TMD) did coIP with Lrp6, indicating that Lrp6-Lypd6

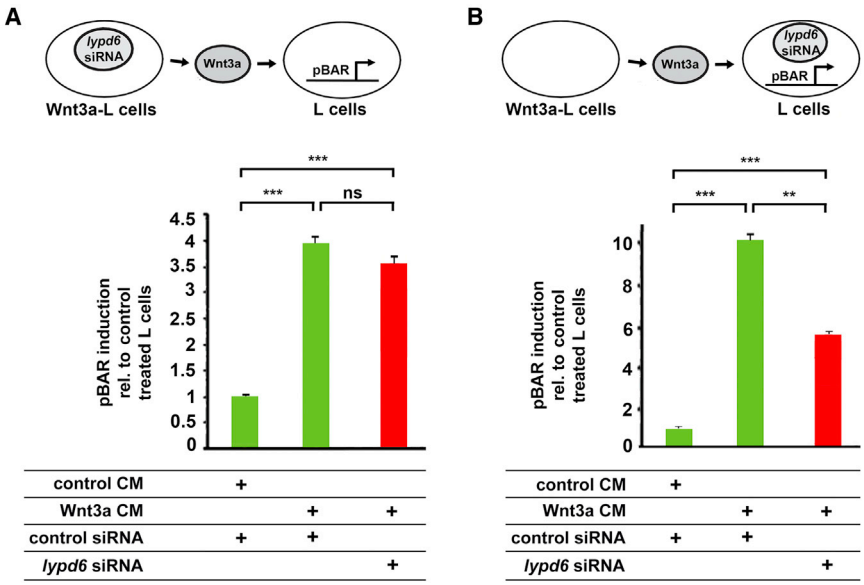

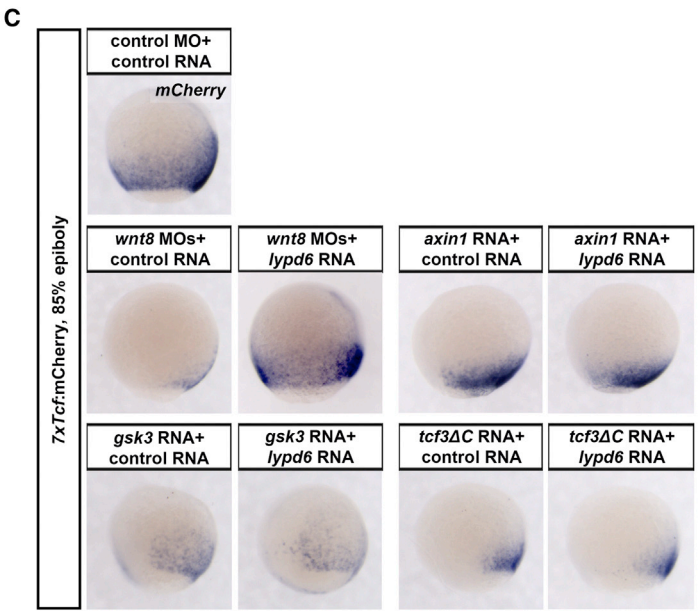

Figure 4. *lypd6* Acts in Wnt-Receiving Cells at the Level of the Wnt Receptor Complex

(A) pBAR luciferase reporter activity in mouse L cells treated with CM produced from control or Wnt3a-producing L cells that were transfected with *lypd6* or control siRNA. Error bars, SEM.

(B) pBAR luciferase reporter activity in Wnt3a CM treated L cells transfected with *lypd6* siRNA. Error bars, SEM.

(C) *lypd6* enhances Wnt/β-catenin signaling upstream of the β-catenin degradation complex. Coinjection of *lypd6* RNA rescues the reduction in reporter activity in *7xTcf*:mCherry embryos caused by *wnt8* MOs (5 ng each, 17/22), but not by RNAs of *axin1* (50 pg, 19/19), *gsk3β* (150 pg, 17/20), or dominant negative *tcf3*, *tcf3ΔC* (125 pg, 23/24) at the 85% epiboly stage.

See also Figure S3.

interaction does not depend on how Lypd6 is localized to the plasma membrane (Figure 5A, lane 8). Purified secreted Lypd6 (spGFP-Lypd6ΔGPI) could be coIPed with the recombinant extracellular domain of Lrp6 (hLrp6-Fc chimera), indicating that Lypd6 and Lrp6 interaction is direct (Figure S4A, lane 2). Dkk1 also coIPed with Lrp6 (Figure S4A, lane 3), whereas secreted GFP (spGFP) did not (lane 1). Furthermore, Lypd6 also interacted with the β-catenin pathway-coupled receptor Frizzled8 (Fz8) as shown by coIP of Lypd6 with immunoprecipitated Fz8 (Figure 5B) and also in the reverse experiment in which Fz8 coIPed with immunoprecipitated Lypd6 (Figure S4B). Interestingly, the Fz8-Lypd6 interaction was strongly enhanced by Wnt3a (compare lanes 3 and 4 in Figure 5B and lanes 3 and 4 in Figure S4B). In contrast, secreted Lypd6 lacking the GPI attachment site could not be coIPed with Wnt8, whereas the Fz8 CRD domain could (Figure S4C). Together, these data suggest that Lypd6 does not act as a Wnt receptor but constitutively and directly interacts with the Wnt coreceptor Lrp6 and is recruited to a Frizzled-containing receptor complex in the presence of Wnt ligands.

Lypd6 Preferentially Partitions into Raft Plasma Membrane Microdomains

GPI-anchored proteins often preferentially partition into liquid-ordered raft membrane microdomains (Friedrichson and Kurzchalia, 1998). To test whether Lypd6 localizes to rafts, we employed giant plasma membrane vesicles (GPMVs), which enable observation of lipid phase separation in plasma membranes isolated from live cells. GPMVs are cell-derived liposomes that can be isolated after chemically induced membrane blebbing and which maintain the lipid and protein diversity of the plasma membrane (Sezgin et al., 2012a). We found that Lypd6 partitioned preferentially into ordered membrane domains in GPMVs derived from CHO cells, which were transfected with spGFP-Lypd6 and stained for the fluorescent lipid marker Fast DiI, which partitions into disordered domains (Figure 5C, 74% ± 6% of spGFP-Lypd6 domains nonoverlapping with DiI). Unlike spGFP-Lypd6, the transmembrane-anchored spGFP-Lypd6ΔGPI-CD44 TMD partitioned into the disordered domains, colocalizing with Fast DiI (5% ± 2% nonoverlapping with DiI, Figure 5D). Likewise, another construct in which the GPI anchor was replaced with the TMD of the human Transferrin receptor (TfR), a nonraft marker protein (spGFP-Lypd6ΔGPI-TfR TMD), localized to disordered domains and was hardly detectable in the ordered phase (Figure 5E, 7% ± 4% nonoverlapping with DiI). As expected, the truncated construct spGFP-Lypd6ΔGPI was not detectable on the surface of GPMVs

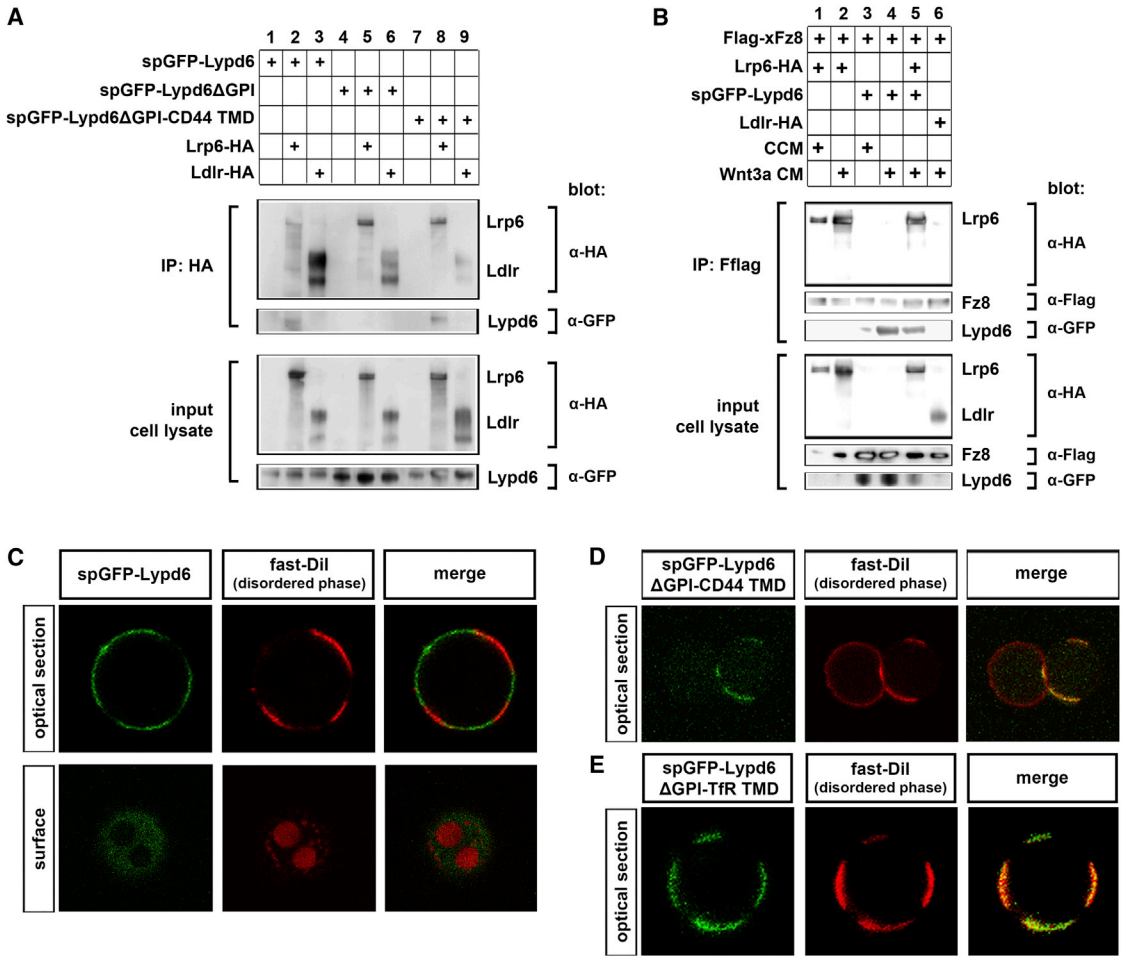

Figure 5. Lypd6 Interacts with Lrp6 and Partitions into Ordered Membrane Domains in Giant Plasma Membrane Vesicles

(A) spGFP-Lypd6 and spGFP-Lypd6ΔGPI-CD44 TMD coIP with Lrp6-HA, but not with Ldlr-HA, in HEK293T cells. spGFP-Lypd6ΔGPI does not coIP with Lrp6-HA or Ldlr-HA.

(B) spGFP-Lypd6 coIPs with Flag-xFz8 in HEK293T cells, and this binding is strongly enhanced by Wnt3a. Flag-xFz8 also binds to Lrp6-HA, which is enhanced by Wnt3a, but does not bind to Ldlr-HA. Lypd6 and Lrp6 still bind to Fz8 when expressed together.

(C–E) Partitioning of various GFP-tagged Lypd6 constructs in giant plasma membrane vesicles (GPMVs) derived from CHO cells. Fast DiI marks the disordered compartments.

See also Figure S4.

(Figure S4D). These data suggest that Lypd6 preferentially partitions into raft membrane domains in live cells.

Mislocalization of Lypd6 to Nonraft Membrane Domains Inhibits Wnt Signaling

As GPI linker replacement with the TfR or the CD44 TMD caused a relocation of Lypd6 from ordered to disordered membrane domains, we asked how this affected Lypd6's ability to modulate Wnt/β-catenin pathway activation. Interestingly, we found that both transmembrane-anchored versions (spGFP-Lypd6ΔGPI-CD44 TMD and spGFP-Lypd6ΔGPI-TfR TMD) significantly reduced the Wnt8-induced pBAR activation in HEK293T cells (Figures 6A and S5A). Furthermore, whereas wild-type spGFP-Lypd6 enhanced the phenotypes induced by overexpression of *wnt8* in zebrafish embryos, the spGFP-Lypd6ΔGPI-TfR TMD had the opposite effect, dampening *wnt8*'s effect (Figure 6B). These data show that constructs in which Lypd6's GPI anchor is replaced by a transmembrane domain act as dominant negatives, indicating that Lypd6 can enhance Wnt signaling only when localized to raft membrane microdomains.

Like other "canonical" Wnt ligands, Wnt8 and Wnt3a trigger interaction of Lrp6 and Frizzled, followed by phosphorylation of Lrp6 at serine and threonine residues in its intracellular domain (Davidson et al., 2005; Zeng et al., 2005) and subsequent internalization of Lrp6 via Caveolin-mediated endocytosis into signaling competent vesicles (Kikuchi and Yamamoto, 2007; Yamamoto et al., 2006). Hence, we asked whether Lypd6 modifies Wnt-induced Lrp6 phosphorylation. In HEK293T cells, Lypd6 transfection slightly increased Lrp6 phosphorylation at S1490 (P-Lrp6) in response to Wnt3a (Figure 6C). Intriguingly, phosphorylation of Lrp6 was inhibited upon expression of spGFP-Lypd6ΔGPI-CD44 TMD or spGFP-Lypd6ΔGPI-TfR TMD, supporting our previous data that both constructs act in a dominant-negative manner (Figures 6C and S5B). Importantly,

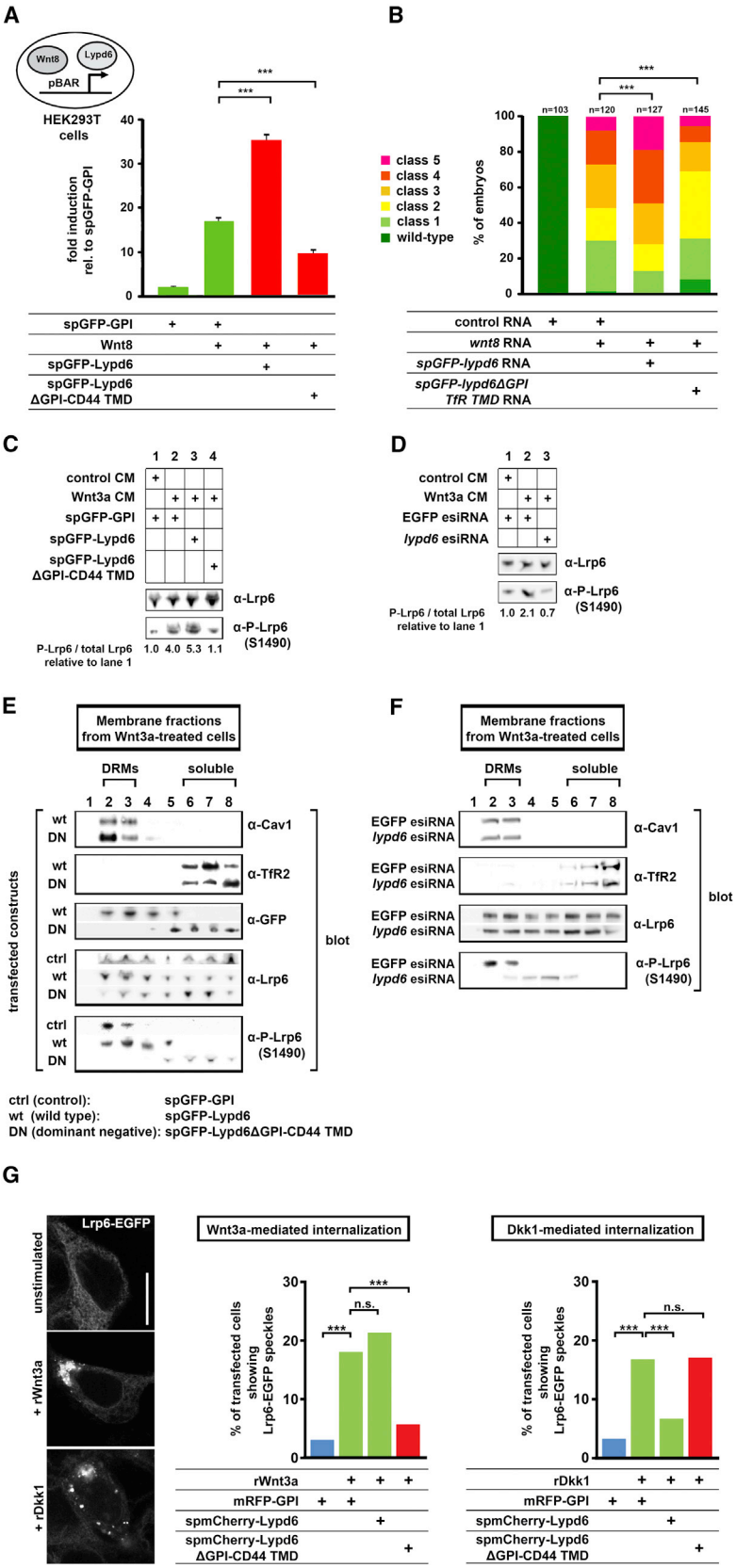

Figure 6. Lypd6 Knockdown or Mislocalization to Nonraft Membrane Domains Shifts Lrp6 Phosphorylation to These Domains and Inhibits Wnt Signaling

(A) pBAR activity in HEK293T cells transfected with Wnt8 (20 ng) plus spGFP-Lypd6 (100 ng) or spGFP-Lypd6ΔGPI-CD44 TMD (95 ng) or equimolar amounts of spGFP-GPI control. Error bars, SEM.

(B) Classes of phenotypes in *wnt8*-overexpressing embryos injected with *wnt8* (20 pg) plus *spGFP-lypd6* (150 pg) or *spGFP-lypd6ΔGPI-TfR TMD* (140 pg) or equimolar amounts of *spGFP-GPI* control RNA. *spGFP-lypd6ΔGPI-TfR TMD* significantly rescues Wnt8-induced phenotypes. Class 5, hyperdorsalization.

(C) spGFP-Lypd6ΔGPI-CD44 TMD reduces Wnt3a-induced phosphorylation of Lrp6 at S1490 in HEK293T cells assayed at 6 hr poststimulation with Wnt3a CM.

(D) *lypd6* esiRNA reduces Wnt3a-induced Lrp6 phosphorylation in HEK293T cells.

(E) Fractionation of plasma membrane derived from HEK293T cells treated with Wnt3a into soluble and detergent-resistant fractions (DRMs). Endogenous TfR2 (a marker for soluble fractions), Caveolin-1 (Cav1, marking DRMs), P-Lrp6 (S1490), Lrp6, and overexpressed GFP in *spGFP-Lypd6* (5 μg) or *spGFP-Lypd6ΔGPI-TfR TMD* (4.6 μg) or control *spGFP-GPI* (2.9 μg) transfected cells were detected by western blotting.

(F) Fractionation of plasma membrane derived from HEK293T cells transfected with 2 μg EGFP control or *lypd6* esiRNAs and treated with Wnt3a CM into soluble and DRM phases.

(G) Imaging and quantification of Wnt3a- or Dkk1-induced Lrp6 speckles in HEK293T cells stably expressing Lrp6-EGFP. Scale bar, 10 μm.

See also Figure S5.

lypd6 knockdown by esiRNA likewise dampened Lrp6 phosphorylation (Figure 6D). We conclude that Lypd6 binds to Lrp6 independently of how it is localized to the plasma membrane but that GPI anchorage of Lypd6 is required for efficient Lrp6 phosphorylation in response to Wnt ligands. Furthermore, Lypd6 mislocalization to nonraft membrane domains can suppress Wnt signaling activation.

Lypd6 Regulates Lrp6 Phosphorylation in Raft Domains

Endogenous Lrp6 is found both in raft and nonraft membrane domains, independent of the presence of Wnt ligands (Yamamoto et al., 2008). Upon Wnt stimulation, phosphorylation of Lrp6, however, occurs preferentially in rafts (Sakane et al., 2010). How raft-specific Lrp6 phosphorylation is regulated remains unknown. Thus, we wondered whether Lypd6 facilitates raft-specific Lrp6 activation.

Association of molecules with the detergent-resistant membrane (DRM) fractions of cell extracts can be used as an indication that such molecules tend to partition into rafts in live cells (Magee and Parmryd, 2003). Using DRM flotation on an *OptiPrep* step gradient, we isolated membranes from Wnt3a-treated HEK293T cells transfected with different Lypd6 constructs and separated the DRMs marked by Caveolin1 (Figure 6E, first panel) from the soluble membranes positive for TfR2 (Figure 6E, second panel). We found that the GPI-anchored spGFP-Lypd6 was enriched in the DRMs, whereas the transmembrane-anchored spGFP-Lypd6ΔGPI-CD44TMD was shifted toward the detergent soluble phase and showed almost no phase overlap with spGFP-Lypd6 (Figure 6E, third panel). Thus, these data are in agreement with our results from GPMVs to indicate that wild-type Lypd6 predominantly localizes to rafts in live cells. Consistent with previously published data (Yamamoto et al., 2008), Lrp6 protein could be detected in both DRMs and soluble fractions in cells transfected with spGFP-GPI control plasmid (Figure 6E, fourth panel). Expression of spGFP-Lypd6 caused a slight shift in Lrp6 distribution toward DRMs, whereas spGFP-Lypd6ΔGPI-CD44 TMD weakly increased Lrp6 abundance in soluble fractions (Figure 6E, fourth panel, see quantification in Figure S5C). Thus, although Lypd6 has a weak ability to recruit Lrp6 to rafts in Wnt-stimulated cells, the modification of Wnt signaling caused by wild-type or dominant-negative Lypd6 likely cannot be explained by effects on Lrp6 recruitment to membrane subdomains.

We then tested whether Lypd6 localization influences Lrp6 phosphorylation in response to Wnt3a treatment. In control spGFP-GPI-transfected cells, phosphorylated Lrp6 could only be detected in the DRM fractions (Figure 6E, fifth panel), in agreement with previous findings (Sakane et al., 2010). Overexpression of wild-type spGFP-Lypd6 slightly increased (1.2-fold) the overall level of P-Lrp6 by inducing Lrp6 phosphorylation in additional fractions, in which the spGFP-Lypd6 construct was present (fractions 4 and 5 in Figure 6E; Figure S5D). In contrast, in membranes isolated from cells transfected with the spGFP-Lypd6ΔGPI-CD44TMD construct, which localized to the soluble membrane fractions, Lrp6 phosphorylation was only detected in the soluble fractions and entirely suppressed in DRMs (Figure 6E; see quantification in Figure S5D). Overall levels of Lrp6 phosphorylation were reduced to 50% when Lypd6 was forced to be expressed in the soluble phases (Figure 6E), consistent with our results from whole-cell lysates. Importantly, knockdown of endogenous *lypd6* likewise caused a shift of Wnt3a-mediated Lrp6 phosphorylation from the DRMs toward the soluble fractions (Figure 6F, fourth panel), while having no influence on the overall Lrp6 distribution on the membrane (Figure 6F, third panel).

These data suggest that Lypd6 controls the site of Lrp6 phosphorylation within the plasma membrane and that it is part of a molecular mechanism that ensures that Lrp6 is phosphorylated in raft domains. In the absence of Lypd6 or when Lypd6 is experimentally mislocalized to soluble membrane fractions, Lrp6 phosphorylation cannot occur in rafts, shifts toward nonraft domains, and is reduced overall (Figure 7).

Raft-specific Lrp6 phosphorylation and subsequent internalization with Caveolin from these domains is thought to be essential for β-catenin pathway activation, whereas Dkk1-mediated Lrp6 internalization from soluble domains with Clathrin prevents pathway activation (Sakane et al., 2010). We thus asked whether Lypd6 has a functional role in Wnt3a- and Dkk1-dependent Lrp6 internalization. In HEK293T cells stably expressing Lrp6-EGFP (Kategaya et al., 2009), Wnt3a-stimulated formation of intracellular speckles containing Lrp6-EGFP (Figure 6G). Whereas overexpression of wild-type spmCherry-Lypd6 did not effect Wnt3a-dependent Lrp6 internalization, dominant-negative spmCherry-Lypd6ΔGPI-CD44 TMD strongly reduced it (Figure 6G). These data suggest that Lrp6 that is forced to be phosphorylated in soluble membrane domains by mislocalization of Lypd6 cannot be internalized in response to Wnt3a and thus does not participate in β-catenin pathway activation.

Dkk1 has been shown to regulate cell-surface availability of Lrp6 by reducing the association of Lrp6 with raft membrane domains and by promoting Clathrin-dependent internalization of Lrp6 into non-raft-associated signaling incompetent compartments (Sakane et al., 2010; Yamamoto et al., 2008). Interestingly, overexpression of wild-type spmCherry-Lypd6 significantly reduced Dkk1-dependent Lrp6 internalization, whereas the dominant-negative spmCherry-Lypd6ΔGPI-CD44 TMD had no effect (Figure 6G). These results suggest that Lypd6 can counteract removal of Lrp6 from raft domains by Dkk1, possibly by promoting raft-association of Lrp6.

Together, these data suggest that Lypd6 is not only required to guarantee Lrp6 phosphorylation in raft domains but also to ensure Wnt-dependent Lrp6 internalization into signaling-competent compartments (Figure 7).

DISCUSSION

This study uncovers a function for Lypd6, a poorly characterized member of the Ly6 family of proteins. Our data suggest that Lypd6 acts as a feedback enhancer of the canonical Wnt/β-catenin signaling pathway by ensuring that the Wnt receptor complex is efficiently activated in rafts, the plasma membrane subcompartment that is competent to transduce the Wnt signal to the interior of the cell. *lypd6* plays essential functions during zebrafish embryogenesis because it is required for efficient *wnt8*-mediated ventralization of the mesoderm and for posteriorization of the neuroectoderm.

Our mechanistic data support the following model for Lypd6's function (Figure 7): in the absence of Wnt (or alternative) ligands,

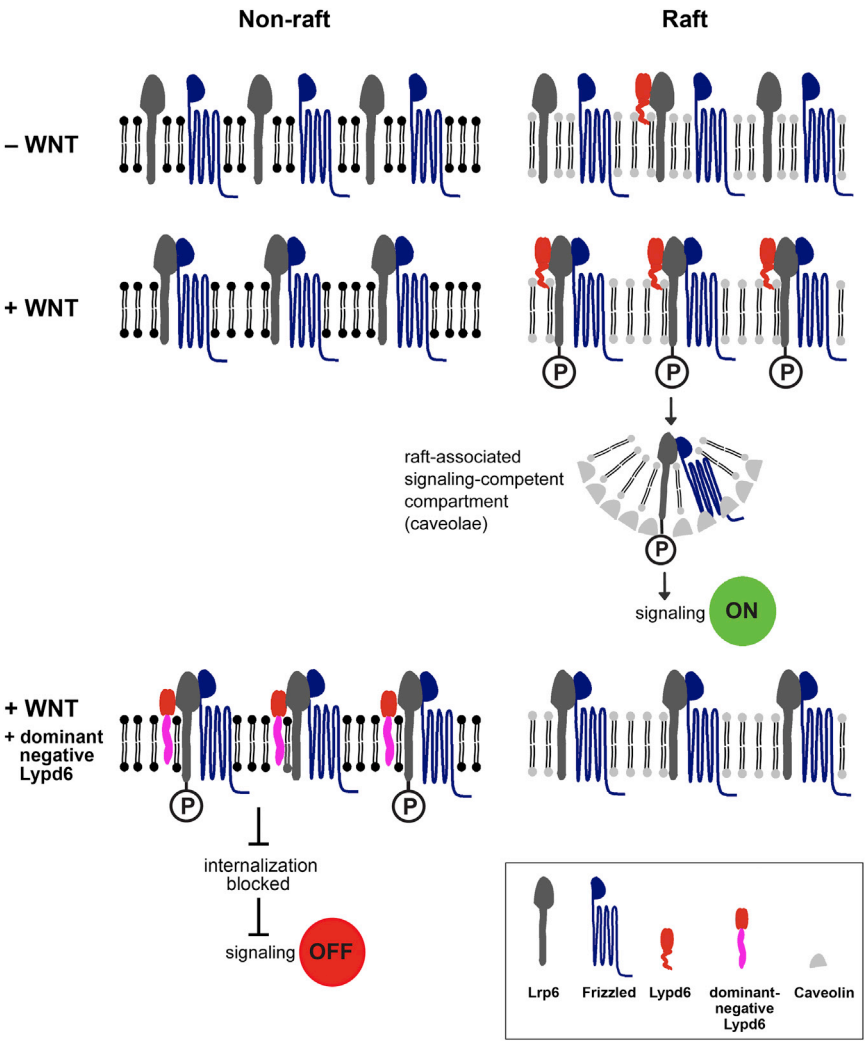

Figure 7. Model of Lypd6 Function as Enhancer of the Wnt/β-Catenin Signaling Pathway

Frizzled and Lrp6 receptors are present in both nonraft and raft membrane domains, while Lypd6, by virtue of its GPI anchor, localizes to rafts, where it directly interacts with Lrp6. In the presence of Wnt ligands, a receptor complex forms, either in all membrane domains (as shown here) or possibly only in rafts. Lypd6 is part of the receptor complex, and because *lypd6* transcription is positively regulated by β-catenin signaling, more Lypd6 localizes to rafts, representing a feedforward mechanism. The presence of Lypd6 in rafts ensures—by an as-yet-unknown mechanism—that the cytoplasmic domain of Lrp6 is only phosphorylated in this membrane domain. Subsequently, the receptor complex is internalized with Caveolin into signaling-competent vesicles, and β-catenin signaling commences. When Lypd6 is mislocalized to nonraft domains (lower panel) by removal of its GPI anchor attachment site and fusion to the transmembrane domain of a protein that localizes to nonrafts, Lrp6 phosphorylation occurs only in nonrafts and at a reduced rate. Under such conditions, the receptor complex cannot be internalized, and β-catenin signaling is blocked. Thus, Lypd6 enhances Wnt/β-catenin signaling by promoting Lrp6 phosphorylation in raft membrane subdomains.

Frizzled receptors and Lrp6 coreceptors are laterally distributed throughout the plasma membrane and found in both nonraft (black) and raft (gray) domains. In contrast, Lypd6, by virtue of its GPI anchor, associates preferentially with the raft domains, where it interacts with Lrp6. In the presence of ligands, Frizzled and Lrp6 form receptor clusters, possibly in all membrane microdomains, while Lypd6 is a component of the receptor complex in the rafts. We propose that Lypd6 is involved in ensuring that Lrp6 phosphorylation only occurs in the raft compartment. Because *lypd6* transcription is under positive feedback regulation by β-catenin signaling, Lypd6 levels rise in the rafts of cells with active signaling, ensuring efficient Lrp6 phosphorylation. Our model further predicts that the active receptor complex is internalized from rafts into signaling-competent Caveolin-rich compartments as has been shown by Yamamoto et al. (2006).

In contrast, when Lypd6 is experimentally forced to localize to nonraft domains of the plasma membrane (dominant-negative Lypd6) or when Lypd6 levels are reduced by knockdown, Lrp6 phosphorylation is reduced and shifted to the nonraft domains (Figure 7). Thus, even though Lrp6 activation in nonraft domains is less efficient than in the rafts, the machinery necessary for Lrp6 phosphorylation must nevertheless be present in nonraft domains. However, phosphorylation of Lrp6 in nonraft domains does not activate intracellular signaling, likely because the receptor complex is not internalized into signaling-competent vesicles from nonraft domains. Clathrin-mediated endocytosis of Lrp6 from nonraft domains is thought to be promoted by Dkk1 and results in inhibition of signaling (Yamamoto et al., 2008). Interestingly, in the presence of dominant-negative Lypd6, Wnt3a does not seem to trigger internalization of the ectopically phosphorylated Lrp6 from nonraft domains via a Clathrin pathway, rather Lrp6 internalization does not occur at all (Figure 7).

How raft-specific Lrp6 phosphorylation is achieved and what mechanistic role Lypd6 plays in this process will have to be elucidated in future studies. Of note, because the clustering of GPI-anchored proteins has been shown to trigger recruitment of kinases at the cytosolic face of the plasma membrane (Harder et al., 1998) and the Lrp6 phosphorylating kinase Ck1γ has been shown to be primarily present in the raft domains in Wnt-stimulated cells (Sakane et al., 2010), Lypd6 might aid in recruitment of Ck1γ and other kinases like Gsk3β to rafts or in regulation of kinase activity in these membrane domains.

In agreement with current concepts of raft membrane domains, it is likely that Lypd6-containing raft domains are small and highly dynamic in the absence of Wnt stimulation. An alternative model to the one presented in Figure 7 would predict that Wnt-induced Frizzled and Lrp6 receptor clustering results

in formation of stable and enlarged rafts containing these clusters. Thus, Wnt receptor clusters might preferentially be present in raft domains. Lypd6 might facilitate this process by virtue of its interaction with Lrp6 and its propensity to associate with rafts via its GPI anchor. However, with the biochemical fractionation methods employed here and by Yamamoto et al. (2006), no change in the ubiquitous distribution of Lrp6 throughout all membrane domains can be detected upon Wnt stimulation. Thus, this alternative model would necessitate the prediction that only a small fraction of Lrp6 molecules participates in receptor clustering in rafts. However, the fact that mislocalized Lypd6 can induce Lrp6 phosphorylation and thus likely also Frizzled-Lrp6 receptor clustering in soluble membrane fractions indicates that receptor clustering does not require the presence of a raft environment. Thus, this finding cannot easily be reconciled with a model of raft-specific receptor clustering.

Membrane rafts play well-characterized roles in the regulation of many signal transduction events by constituting a stage for clustering of ligands, receptors, and various signaling modifiers (Simons and Toomre, 2000). Raft association can promote receptor signaling, for example, signaling activated by Toll-like receptors, T cell receptors, and immunoglobulin E, by promoting receptor association with activating kinases or by shielding them from deactivating phosphatases (Fessler and Parks, 2011; Kusumi et al., 2012). However, rafts have also been proposed to interfere with signaling of TGF-β receptors, by promoting receptor degradation (Chen et al., 2007). A series of elegant studies by Yamamoto et al. (2006) has revealed the importance of membrane rafts in activation of Wnt/β-catenin signaling, by showing that Lrp6 phosphorylation occurs in rafts and that subsequent internalization into caveolae is essential for signaling (Sakane et al., 2010; Yamamoto et al., 2006, 2008). Recently, we have suggested that Waif1a, a feedback inhibitor of β-catenin signaling, acts by suppressing Lrp6 internalization into signaling-competent vesicles (Kagermeier-Schenk et al., 2011). In contrast, the secreted pathway inhibitor Dkk1 removes Lrp6 from rafts and promotes its internalization with Clathrin (Sakane et al., 2010; Yamamoto et al., 2008). It will be interesting to see whether other Wnt modifiers target Lrp6 distribution within the plasma membrane.

Modulation of receptor-mediated signaling is a function shared between Lypd6 and other members of the Ly6 family. The GPI-anchored Ly6 E, also called Tsa-1 or Sca-2, has been suggested to be required for T-cell-receptor phosphorylation and signaling (Saitoh et al., 1995). It would be interesting to test whether this involves a similar mechanism to the one proposed here for Lypd6, namely, raft-specific receptor activation. CD59, which localizes to rafts due to its GPI anchor, has been proposed to stimulate human T-cell-receptor signaling via activation of kinases, although loss-of-function studies in mice rather demonstrate an inhibitory effect on T cell signaling (Kimberley et al., 2007; Murray and Robbins, 1998).

Other membrane raft-associated GPI-anchored proteins have also been proposed to modulate signaling pathways by causing a rearrangement of signaling components in the plasma membrane. CD48, an immunomodulatory molecule found on various hematopoietic cells, interacts with the natural killer cell receptor 2B4 and appears to activate Src tyrosine kinases, despite lacking an intracellular domain, which implies that it acts by altering distribution of receptors and kinases in the membrane (Elishmereni and Levi-Schaffer, 2011). Likewise, CD48 has been reported to enhance raft-dependent association of the T cell receptor with the actin cytoskeleton and its tyrosine phosphorylation (Moran and Miceli, 1998). Similarly, stimulation of neurons with the glial-cell-derived neurotrophic factor (Gdnf) promotes the GPI-linked Gdnf receptor-α1 (Gfrα1) to recruit the Ret tyrosine kinase receptor to raft domains, which activates signaling (Tansey et al., 2000).

In vivo functions of *lypd6* have only been incompletely studied. Mouse and human *lypd6* are strongly expressed in the adult central nervous system (Darvas et al., 2009; Zhang et al., 2010). Transgenic mice ubiquitously expressing small hairpin RNA targeting *lypd6* produced few offspring, indicating a defect in gametogenesis or embryonic lethality, but a potential embryonic phenotype has not been characterized (Darvas et al., 2009). Transgenic *lypd6* overexpression in vivo and knockdown in isolated trigeminal ganglion neurons revealed that mouse *lypd6* positively regulates Ca^{2+} flux through nAChRs (Darvas et al., 2009). Interestingly, modulation of nAChRs appears to be a function common to several three finger proteins (the superfamily Ly6 proteins belong to), because the secreted Ly6 family members Slurp1 and Slurp2 are nAChR ligands that regulate epidermal homeostasis (Kong and Park, 2012), whereas the structurally related snake α-neurotoxins are potent antagonists of nAChRs (Tsetlin, 1999). Our study defines an essential function for a Ly6 family member during early vertebrate development. We found that *lypd6* is essential for efficient Wnt/β-catenin signaling during gastrulation, where it is broadly expressed. However, at later stages of development, *lypd6* is not expressed in all tissues known to have active Wnt signaling. This raises the question of whether other molecules, possibly from the Ly6 family or from other GPI-anchored protein classes, fulfill Lypd6's role as regulator of raft-specific Lrp6 phosphorylation in these tissues. It will also be interesting to test whether Lypd6 has roles in β-catenin-independent Wnt signaling.

Our study reveals that the activation of Wnt pathway components in specific plasma membrane microdomains is a target for cellular modifiers of the pathway. Future studies will not only elucidate the molecular mechanisms underlying such regulation but will also reveal whether these principles could be adopted for therapeutic interventions.

EXPERIMENTAL PROCEDURES

Additional experimental procedures are described in the Supplemental Experimental Procedures.

Transgenic Fish Lines

Outcrosses of the following transgenic lines were heat shocked and identified as described previously (Kagermeier-Schenk et al., 2011): Tg(*hsp70l*:wnt8a-GFP)^{w34} (Weidinger et al., 2005), Tg(*hsp70l*:dkk1-GFP)^{w32} (Stoick-Cooper et al., 2007), and Tg(*hsp70l*:Mmu.Axin1-YFP)^{w35} (Kagermeier-Schenk et al., 2011). The *7xTcfF-Xla.Siam:*nlsmCherry^{ia}transgenic line was used as a reporter of Wnt/β-catenin signaling (Moro et al., 2012).

Morpholino Oligonucleotides, Microinjection, and Whole-Mount In Situ Hybridization

Capped sense RNA was synthesized in vitro using mMessage mMachine kits (Ambion). RNA and/or morpholinos were injected into the cytoplasm of one-cell stage zebrafish embryos using standard procedures. Zebrafish embryos

were fixed at the indicated stages, and mRNA whole-mount in situ hybridization (WMISH) was performed as described previously (Jowett and Lettice, 1994). *Xenopus* embryos were staged in accordance with Nieuwkoop and Faber's procedure, and WMISH was performed as described previously (Hemmati-Brivanlou et al., 1990). The *lypd6* MO has the sequence 5′-CCATGA GAGGCCAGGGCTCCATAAT-3′, *wnt8.1* (ORF1), and *wnt8.2*(ORF2) MOs were used as published previously (Lekven et al., 2001).

Western Blot Analysis and Immunoprecipitation

Samples were dissolved in SDS gel-loading buffer that contained β-mercaptoethanol, separated by SDS-PAGE on 10% Bis-TrisNuPage precast gels (Life Technologies), and transferred to polyvinylidene fluorid membrane (Life Technologies). The following antibodies were used: mouse anti-cMyc monoclonal (Life Technologies, 1:2,000), rabbit anti-GFP (Abcam, 1:2,000), goat anti-GFP antibody (MPI-CBG Dresden Antibody Facility, 1:1,000), rabbit anti-Flag (Sigma, 1:1,000), rabbit anti-HA (Abcam, 1:2,000), rabbit anti-Phospho-Lrp6 (Ser1490, Cell Signaling, 1:1,000), rabbit anti-LRP (Cell Signaling, 1:1,000), rabbit anti-TfR2 (Abcam, 1:2,000), and mouse anti-Caveolin1 (BD Transduction Laboratories, 1:2,000). Immunoprecipitation (IP) experiments were performed as described previously (Kagermeier-Schenk et al., 2011).

Secretion Assay

HEK293T cells were transfected with either spGFP-Lypd6 (150 ng) or spGFP-Lypd6ΔGPI (140 ng) along with equimolar amounts of spGFP-GPI and spGFP as controls, respectively. At 24 hr posttransfection cells were treated with phosphatidylinositol-specific phospholipase C (PipIC, 1 U/ml) for 12 hr at 37°C. Conditioned media were collected and concentrated using a centrifugal evaporator. Cells were lysed with passive lysis buffer (Promega), and lysates and media were subjected to anti-GFP western blotting.

lypd6 siRNAs and esiRNA

Mouse *lypd6* was knocked down in control- or Wnt3a-expressing L cells via reverse transfection with 100 nmol StealthTM siRNA (5′-GCCACATTTGCTAC CACATCACCTA-3′, Life Technologies) or equimolar amounts of standard medium GC-negative control siRNA using Lipofectamine RNAiMAX transfection reagent (Life Technologies). Cells were retransfected with the same amount of siRNA after 24 hr. For the Wnt production assay, conditioned media were collected from transfected cells, and pBAR assays were performed as described in the Supplemental Experimental Procedures. For the Wnt reception assay, siRNA-transfected cells were transfected with pBAR and pGL4.73 hRLuc/SV40, and Wnt3a CM stimulation and dual luciferase assays were performed 48 hr later.

Transfection and luciferase assays in HEK293T or RKO cells with 100 nmole human *lypd6* StealthTM siRNA (5′-GTCCCGAGACTTCACAGTGAAAGAC-3′, Life Technologies) or standard medium GC-negative control siRNA were performed as described above.

Human *lypd6* was knocked down in HEK293T cells via reverse transfection with 2 μg of esiRNA (5′-CCATCTGCCCTCCATAGAAAAATGTCTCTGGCTCA TAAAATGAGACTCCCTCAGGGAC-3′, Sigma-Aldrich) or equimolar amounts of standard negative control EGFP esiRNA (Sigma-Aldrich) using Lipofectamine RNAiMAX transfection reagent.

Preparation of Giant Plasma Membrane Vesicles

Giant plasma membrane vesicles (GPMVs) were prepared as previously described (Sezgin et al., 2012a), with minor modifications. Chinese hamster ovary (CHO) or HEK293T cells were cultured on fibronectin-coated petri dishes, in alpha MEM or Dulbecco's modified Eagle's medium (DMEM) supplemented with 10% fetal calf serum to 70%–80% of confluence. GPMVs were isolated by chemically induced cell blebbing with either 25 mM PFA plus 2 mM DTT or 2 mM *N*-ethyl maleimide (NEM) in GPMV buffer (150 mM NaCl, 10 mM HEPES, and 2 mM $CaCl_2$ [pH 7.4]) for 1.5 hr at 37°C. GPMVs were gently collected to avoid cell detachments. The fluorescent lipid marker Fast DiI (Life Technologies) was added to GPMVs at a final concentration of 0.1 μM. The stained GPMVs were imaged at 5°C (NEM GPMVs) or at 10°C (PFA/DTT GPMVs), using a Zeiss LSM 510 confocal microscope. As no difference was observed between the two preparations, we used PFA/DTT vesicles for further analysis. To calculate the extent of localization of GFP-tagged proteins to ordered domains, GPMVs that displayed ordered and disordered domains at opposite sides were used. Then a line scan through both ordered and disordered domains was used to quantify the fluorescence intensity in different domains. Background intensity values obtained from pixels outside the vesicles were subtracted, and a relative raft partitioning index was calculated by dividing the fluorescent intensity in the ordered phase by the sum of the fluorescence intensities in ordered and disordered domains (Sezgin et al., 2012b). Average partitioning index was obtained from at least ten individual measurements.

DRM Flotation

HEK293T cells seeded into 10 cm culture dishes were transiently transfected with spGFP-Lypd6, spGFP-Lypd6ΔGPI-CD44 TMD, or spGFP-GPI as control, stimulated with Wnt3a conditioned media for 6 hr 2 days after transfection and washed twice with 1X cold TNE buffer (50 mM Tris [pH 7.4], 150 mM NaCl, and 2 mM EDTA). Cells were harvested with 1X TNE containing protease inhibitor cocktail (PIC, Sigma) and phosphatase inhibitors (PI, Calbiochem) and pelleted at 1,000 rpm for 5 min at 4°C. Pellets were resuspended in 400 μl TNE+PIC+PI containing 1% Triton X-100 and lysed by passing through a 25G needle 15–20 times; pellets were incubated on ice for 30 min. Samples were spun at 13,200 rpm at 4°C for 10 min. Gradients were prepared by mixing 320 μl of the solubilized sample with 640 μl OptiPrep stock (60%) (Sigma) and overlaying with 1,680 μl 30% OptiPrep (in TNE+PIC+PI) and 720 μl 5% OptiPrep. Samples were ultracentrifuged using an MLS-50 rotor in an Optima MAX ultracentrifuge at 45,000 rpm for 4 hr at 4°C, and eight fractions of 400 μl each were collected. Proteins were precipitated in 10% TCA at max speed on a table-top centrifuge for 1 hr at 4°C. Pellets were resuspended in sample loading buffer with β-mercaptoethanol and processed for western blotting.

Lrp6 Internalization Assays

The internalization assay of Lrp6 in HEK293T cells stably expressing Lrp6-EGFP (Biechele and Moon, 2008) in response to Dkk1 or Wnt3a was performed as follows. At 24 hr after transfection with mRFP-GPI, spmCherry-Lypd6, or spmCherry-Lypd6ΔGPI-CD44 TMD, HEK293T cells were incubated at 4°C for 30 min with binding medium (DMEM, 20 mM HEPES [pH 7.5], 0.1% bovine serum albumin) and subsequently incubated at 4°C for 60 min with binding medium supplemented with 200 ng/ml recombinant mouse Wnt3a (rWnt3a) or human Dkk1 (rDkk1) (R&D Systems). Afterward, internalization was initiated by adding warm DMEM supplemented with 200 ng rWnt3a or rDkk1, and dishes were transferred to a heated chamber (37°C, 5% CO_2) for 30 min. Cells were fixed, stained with DAPI, and viewed using a confocal microscope (Leica SP5).

Statistics

Significance was tested using Student's t test (Figures 1B, 2C, 3B, 3E, 4A, 4B, 6A, and 6G; Figures S2G and S2H, S3A–S3F, and S5A), chi-square test (Figures 2B, 2E, 6B, 6G, and S2B), or nonparametric Mann-Whitney rank-sum test (Figure S2D). pBAR reporter data are averages from triplicate transfections; one representative result from at least three independent experiments is shown (Figures 2C, 4A, 4B, and 6A; Figures S3D–S3F and S5A). *** indicates $p < 0.001$, ** $p < 0.01$, and * $p < 0.05$; n.s. nonsignificant. Error bars represent SEM.

ACCESSION NUMBERS

The GenBank accession number for the partial *Xenopus laevis lypd6* complementary DNA reported in this paper is KF042353.

SUPPLEMENTAL INFORMATION

Supplemental Information includes Supplemental Experimental Procedures and five figures and can be found with this article online at http://dx.doi.org/10.1016/j.devcel.2013.07.020.

ACKNOWLEDGMENTS

We thank Christa Haase for technical assistance, Marika Fischer and Jitka Michling for fish care, Akira Kikuchi and Ronald Dirkx for suggestions on the

DRM flotation protocol, Michael Brand for the spGFP, spGFP-GPI, and mRFP-GPI plasmids, and Christof Niehrs for the pCS-Nflag-xfz8 plasmid. Research for this project in the Weidinger laboratory is supported by a grant from the Deutsche Forschungsgemeinschaft (DFG) (WE 4223/4-1). E.S. and P.S. were supported by a DFG grant (SO-818/1-1).

Received: December 25, 2012
Revised: May 23, 2013
Accepted: July 29, 2013
Published: August 26, 2013

REFERENCES

Angers, S., and Moon, R.T. (2009). Proximal events in Wnt signal transduction. Nat. Rev. Mol. Cell Biol. *10*, 468–477.

Bamezai, A. (2004). Mouse Ly-6 proteins and their extended family: markers of cell differentiation and regulators of cell signaling. Arch. Immunol. Ther. Exp. (Warsz.) *52*, 255–266.

Biechele, T.L., and Moon, R.T. (2008). Assaying beta-catenin/TCF transcription with beta-catenin/TCF transcription-based reporter constructs. Methods Mol. Biol. *468*, 99–110.

Chen, C.L., Liu, I.H., Fliesler, S.J., Han, X., Huang, S.S., and Huang, J.S. (2007). Cholesterol suppresses cellular TGF-beta responsiveness: implications in atherogenesis. J. Cell Sci. *120*, 3509–3521.

Clevers, H. (2006). Wnt/beta-catenin signaling in development and disease. Cell *127*, 469–480.

Darvas, M., Morsch, M., Racz, I., Ahmadi, S., Swandulla, D., and Zimmer, A. (2009). Modulation of the Ca2+ conductance of nicotinic acetylcholine receptors by Lypd6. Eur. Neuropsychopharmacol. *19*, 670–681.

Davidson, G., Wu, W., Shen, J., Bilic, J., Fenger, U., Stannek, P., Glinka, A., and Niehrs, C. (2005). Casein kinase 1 gamma couples Wnt receptor activation to cytoplasmic signal transduction. Nature *438*, 867–872.

Elishmereni, M., and Levi-Schaffer, F. (2011). CD48: A co-stimulatory receptor of immunity. Int. J. Biochem. Cell Biol. *43*, 25–28.

Fessler, M.B., and Parks, J.S. (2011). Intracellular lipid flux and membrane microdomains as organizing principles in inflammatory cell signaling. J. Immunol. *187*, 1529–1535.

Friedrichson, T., and Kurzchalia, T.V. (1998). Microdomains of GPI-anchored proteins in living cells revealed by crosslinking. Nature *394*, 802–805.

Gumley, T.P., McKenzie, I.F., and Sandrin, M.S. (1995). Tissue expression, structure and function of the murine Ly-6 family of molecules. Immunol. Cell Biol. *73*, 277–296.

Harder, T., Scheiffele, P., Verkade, P., and Simons, K. (1998). Lipid domain structure of the plasma membrane revealed by patching of membrane components. J. Cell Biol. *141*, 929–942.

Hemmati-Brivanlou, A., Frank, D., Bolce, M.E., Brown, B.D., Sive, H.L., and Harland, R.M. (1990). Localization of specific mRNAs in Xenopus embryos by whole-mount in situ hybridization. Development *110*, 325–330.

Jowett, T., and Lettice, L. (1994). Whole-mount in situ hybridizations on zebrafish embryos using a mixture of digoxigenin- and fluorescein-labelled probes. Trends Genet. *10*, 73–74.

Kagermeier-Schenk, B., Wehner, D., Ozhan-Kizil, G., Yamamoto, H., Li, J., Kirchner, K., Hoffmann, C., Stern, P., Kikuchi, A., Schambony, A., and Weidinger, G. (2011). Waif1/5T4 inhibits Wnt/β-catenin signaling and activates noncanonical Wnt pathways by modifying LRP6 subcellular localization. Dev. Cell *21*, 1129–1143.

Kategaya, L.S., Changkakoty, B., Biechele, T., Conrad, W.H., Kaykas, A., Dasgupta, R., and Moon, R.T. (2009). Bili inhibits Wnt/beta-catenin signaling by regulating the recruitment of axin to LRP6. PLoS ONE *4*, e6129.

Kikuchi, A., and Yamamoto, H. (2007). Regulation of Wnt signalling by receptor-mediated endocytosis. J. Biochem. *141*, 443–451.

Kim, N.C., and Marqués, G. (2012). The Ly6 neurotoxin-like molecule target of wit regulates spontaneous neurotransmitter release at the developing neuromuscular junction in Drosophila. Dev. Neurobiol. *72*, 1541–1558.

Kimberley, F.C., Sivasankar, B., and Paul Morgan, B. (2007). Alternative roles for CD59. Mol. Immunol. *44*, 73–81.

Kimelman, D., and Xu, W. (2006). beta-catenin destruction complex: insights and questions from a structural perspective. Oncogene *25*, 7482–7491.

Kong, H.K., and Park, J.H. (2012). Characterization and function of human Ly-6/uPAR molecules. BMB Rep. *45*, 595–603.

Kusumi, A., Fujiwara, T.K., Morone, N., Yoshida, K.J., Chadda, R., Xie, M., Kasai, R.S., and Suzuki, K.G. (2012). Membrane mechanisms for signal transduction: the coupling of the meso-scale raft domains to membrane-skeleton-induced compartments and dynamic protein complexes. Semin. Cell Dev. Biol. *23*, 126–144.

Lekven, A.C., Thorpe, C.J., Waxman, J.S., and Moon, R.T. (2001). Zebrafish wnt8 encodes two wnt8 proteins on a bicistronic transcript and is required for mesoderm and neurectoderm patterning. Dev. Cell *1*, 103–114.

Logan, C.Y., and Nusse, R. (2004). The Wnt signaling pathway in development and disease. Annu. Rev. Cell Dev. Biol. *20*, 781–810.

MacDonald, B.T., Tamai, K., and He, X. (2009). Wnt/beta-catenin signaling: components, mechanisms, and diseases. Dev. Cell *17*, 9–26.

Magee, A.I., and Parmryd, I. (2003). Detergent-resistant membranes and the protein composition of lipid rafts. Genome Biol. *4*, 234.

Moran, M., and Miceli, M.C. (1998). Engagement of GPI-linked CD48 contributes to TCR signals and cytoskeletal reorganization: a role for lipid rafts in T cell activation. Immunity *9*, 787–796.

Moro, E., Ozhan-Kizil, G., Mongera, A., Beis, D., Wierzbicki, C., Young, R.M., Bournele, D., Domenichini, A., Valdivia, L.E., Lum, L., et al. (2012). In vivo Wnt signaling tracing through a transgenic biosensor fish reveals novel activity domains. Dev. Biol. *366*, 327–340.

Murray, E.W., and Robbins, S.M. (1998). Antibody cross-linking of the glycosylphosphatidylinositol-linked protein CD59 on hematopoietic cells induces signaling pathways resembling activation by complement. J. Biol. Chem. *273*, 25279–25284.

Niehrs, C., and Shen, J. (2010). Regulation of Lrp6 phosphorylation. Cell. Mol. Life Sci. *67*, 2551–2562.

Pilon, N., Oh, K., Sylvestre, J.R., Bouchard, N., Savory, J., and Lohnes, D. (2006). Cdx4 is a direct target of the canonical Wnt pathway. Dev. Biol. *289*, 55–63.

Saitoh, S., Kosugi, A., Noda, S., Yamamoto, N., Ogata, M., Minami, Y., Miyake, K., and Hamaoka, T. (1995). Modulation of TCR-mediated signaling pathway by thymic shared antigen-1 (TSA-1)/stem cell antigen-2 (Sca-2). J. Immunol. *155*, 5574–5581.

Sakane, H., Yamamoto, H., and Kikuchi, A. (2010). LRP6 is internalized by Dkk1 to suppress its phosphorylation in the lipid raft and is recycled for reuse. J. Cell Sci. *123*, 360–368.

Sezgin, E., Kaiser, H.J., Baumgart, T., Schwille, P., Simons, K., and Levental, I. (2012a). Elucidating membrane structure and protein behavior using giant plasma membrane vesicles. Nat. Protoc. *7*, 1042–1051.

Sezgin, E., Levental, I., Grzybek, M., Schwarzmann, G., Mueller, V., Honigmann, A., Belov, V.N., Eggeling, C., Coskun, U., Simons, K., and Schwille, P. (2012b). Partitioning, diffusion, and ligand binding of raft lipid analogs in model and cellular plasma membranes. Biochim. Biophys. Acta *1818*, 1777–1784.

Simons, K., and Toomre, D. (2000). Lipid rafts and signal transduction. Nat. Rev. Mol. Cell Biol. *1*, 31–39.

Stoick-Cooper, C.L., Weidinger, G., Riehle, K.J., Hubbert, C., Major, M.B., Fausto, N., and Moon, R.T. (2007). Distinct Wnt signaling pathways have opposing roles in appendage regeneration. Development *134*, 479–489.

Syed, M.H., Krudewig, A., Engelen, D., Stork, T., and Klämbt, C. (2011). The CD59 family member Leaky/Coiled is required for the establishment of the blood-brain barrier in Drosophila. J. Neurosci. *31*, 7876–7885.

Tansey, M.G., Baloh, R.H., Milbrandt, J., and Johnson, E.M., Jr. (2000). GFRalpha-mediated localization of RET to lipid rafts is required for effective downstream signaling, differentiation, and neuronal survival. Neuron *25*, 611–623.

Tsetlin, V. (1999). Snake venom alpha-neurotoxins and other 'three-finger' proteins. Eur. J. Biochem. *264*, 281–286.

Weidinger, G., Thorpe, C.J., Wuennenberg-Stapleton, K., Ngai, J., and Moon, R.T. (2005). The Sp1-related transcription factors sp5 and sp5-like act downstream of Wnt/beta-catenin signaling in mesoderm and neuroectoderm patterning. Curr. Biol. *15*, 489–500.

Yamaguchi, T.P. (2001). Heads or tails: Wnts and anterior-posterior patterning. Curr. Biol. *11*, R713–R724.

Yamamoto, H., Komekado, H., and Kikuchi, A. (2006). Caveolin is necessary for Wnt-3a-dependent internalization of LRP6 and accumulation of beta-catenin. Dev. Cell *11*, 213–223.

Yamamoto, H., Sakane, H., Yamamoto, H., Michiue, T., and Kikuchi, A. (2008). Wnt3a and Dkk1 regulate distinct internalization pathways of LRP6 to tune the activation of beta-catenin signaling. Dev. Cell *15*, 37–48.

Zeng, X., Tamai, K., Doble, B., Li, S., Huang, H., Habas, R., Okamura, H., Woodgett, J., and He, X. (2005). A dual-kinase mechanism for Wnt co-receptor phosphorylation and activation. Nature *438*, 873–877.

Zhang, Y., Lang, Q., Li, J., Xie, F., Wan, B., and Yu, L. (2010). Identification and characterization of human LYPD6, a new member of the Ly-6 superfamily. Mol. Biol. Rep. *37*, 2055–2062.